JOURNAL OF MATERIALS SCIENCE 36 (2001) 1315–1324

Review
Functional properties of cement-matrix composites

D. D. L. CHUNG
Composite Materials Research Laboratory, State University of New York at Buffalo, Buffalo, NY 14260-4400, USA
E-mail: ddLchung@ACSU.buffalo.edu

The functional properties of cement-matrix composites are reviewed. The functions include strain sensing, damage sensing, temperature sensing, thermal control, vibration reduction and radio wave reflection. The functions are rendered by the use of admixtures, such as short carbon fibers, short steel fibers and silica fume.

1. Introduction

As the demand for the functions of a structure increases, the functional properties of structural materials are receiving more and more attention. The goal of much current research in structural materials is the development of multifunctional materials which are attractive in both structural and functional properties. Multifunctionality means killing two or more birds with one stone, thus saving cost and simplifying design. Instead of using an attached or embedded device to provide the structure with a certain function (such as sensing), the structural material is exploited for that function. The consequence is reduced cost, enhanced durability, increased functional volume and absence of mechanical property degradation, which occurs in the case of embedded devices.

Concrete (a cement-matrix composite) is the dominant structural material for the civil infrastructure. Much attention has been given to the structural properties of cement-matrix composites, but relatively little attention has been given to the functional properties. This paper reviews the functional properties of cement-matrix composites. The functions addressed include strain sensing, damage sensing, temperature sensing, thermal control, vibration reduction and radio wave reflection.

2. Cement-matrix composites for strain sensing

The electrical resistance of strain sensing concrete (without embedded or attached sensors) changes reversibly with strain, such that the gage factor (fractional change in resistance per unit strain) is up to 700 under compression or tension [1–17]. The resistance (DC/AC) increases reversibly upon tension and decreases reversibly upon compression, due to fiber pull-out upon microcrack opening (<1 μm) and the consequent increase in fiber-matrix contact resistivity. The concrete contains as low as 0.2 vol.% short carbon fibers, which are preferably those that have been surface treated. The fibers do not need to touch one another in the composite. The treatment improves the wettability with water. The presence of a large aggregate decreases the gage factor, but the strain sensing ability remains sufficient for practical use. Strain sensing concrete works even when data acquisition is wireless (involving telemetry). The applications include structural vibration control and traffic monitoring.

Fig. 1a [11] shows the fractional change in resistivity along the stress axis as well as the strain during repeated compressive loading at an increasing stress amplitude for carbon-fiber latex cement paste at 28 days of curing. Fig. 1b [11] shows the corresponding variation of stress and strain during the repeated compressive loading. The strain varies linearly with the stress up to the highest stress amplitude (Fig. 1b). The strain returns to zero at the end of each cycle of loading. The resistivity decreases upon loading in every cycle (due to fiber push-in) and increases upon unloading in every cycle (due to fiber pull-out). The resistivity has a net increase after the first cycle, due to damage. Little further damage occurs in subsequent cycles, as shown by the resistivity after unloading not increasing much after the first cycle. The greater the strain amplitude, the more is the resistivity decrease during loading, although the resistivity and strain are not linearly related. The effects of Fig. 1 were similarly observed in carbon-fiber silica-fume cement paste at 28 days of curing.

Figs 2 and 3 [12] show the fractional changes in the longitudinal and transverse resistivities respectively for carbon-fiber silica-fume cement paste at 28 days of curing during repeated unaxial tensile loading at increasing strain amplitudes. The strain essentially returns to zero at the end of each cycle, indicating elastic deformation. The longitudinal strain is positive (i.e., elongation); the transverse strain is negative (i.e., shrinkage due to the Poisson Effect). Both longitudinal and transverse resistivities increase reversibly upon uniaxial tension. The reversibility of both strain and resistivity

0022–2461

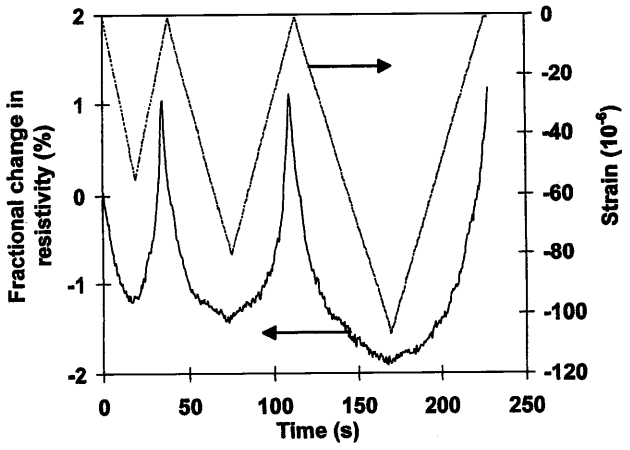

(a)

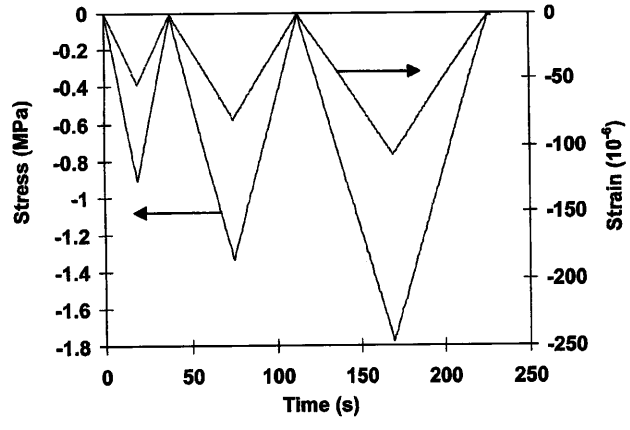

(b)

Figure 1 Variation of the fractional change in volume electrical resistivity with time (a), of the stress with time (b), and of the strain (negative for compressive strain) with time (a,b) during dynamic compressive loading at increasing stress amplitudes within the elastic regime for carbon-fiber latex cement paste at 28 days of curing.

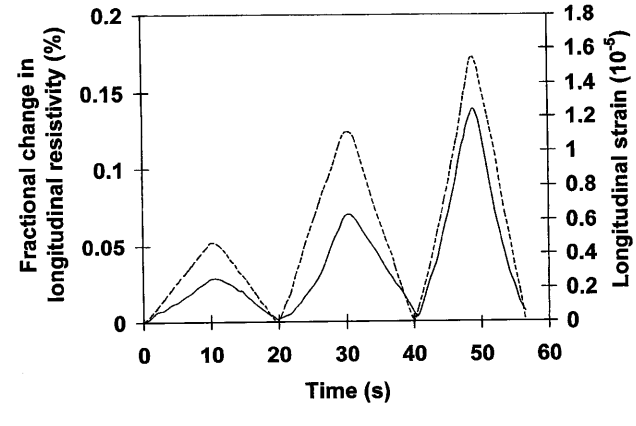

Figure 2 Variation of the fractional change in longitudinal electrical resistivity with time (solid curve) and of the strain with time (dashed curve) during dynamic uniaxial tensile loading at increasing stress amplitudes within the elastic regime for carbon-fiber silica-fume cement paste.

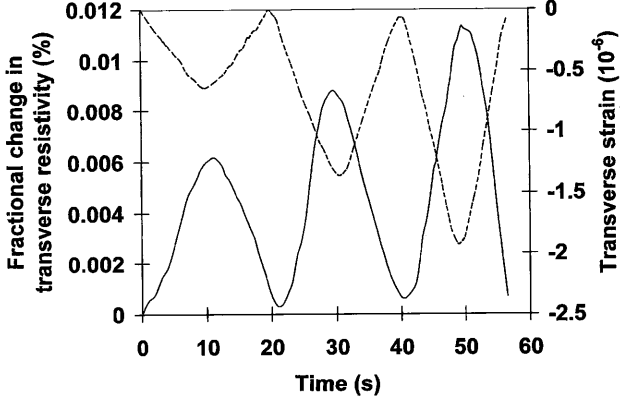

Figure 3 Variation of the fractional change in transverse electrical resistivity with time (solid curve) and of the strain with time (dashed curve) during dynamic uniaxial tensile loading at increasing stress amplitudes within the elastic regime for carbon-fiber silica-fume cement paste.

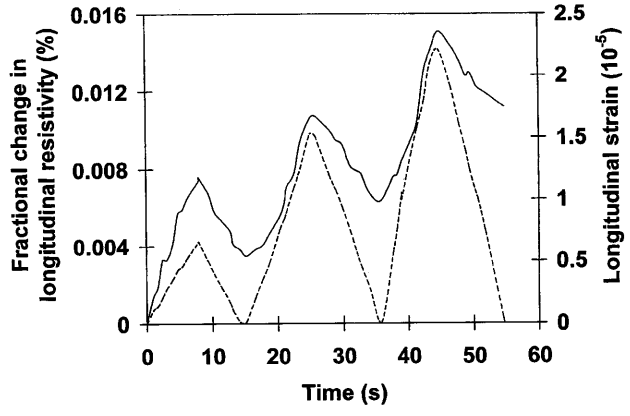

Figure 4 Variation of the fractional change in longitudinal electrical resistivity with time (solid curve) and of the strain with time (dashed curve) during dynamic uniaxial tensile loading at increasing stress amplitudes within the elastic regime for silica-fume cement paste.

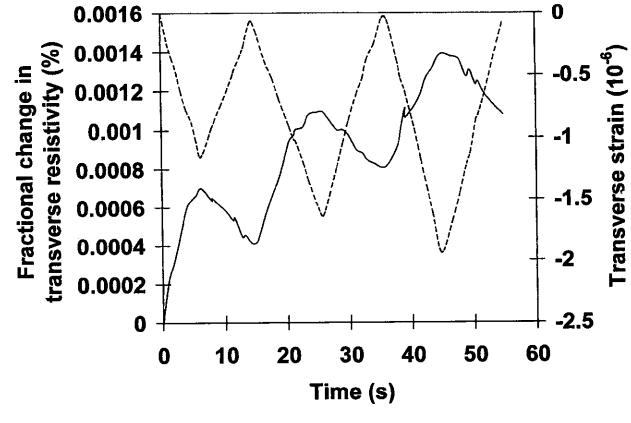

Figure 5 Variation of the fractional change in transverse electrical resistivity with time (solid curve) and of the strain with time (dashed curve) during dynamic uniaxial tensile loading at increasing stress amplitudes within the elastic regime for silica-fume cement paste.

is more complete in the longitudinal direction than the transverse direction. The gage factor is 89 and −59 for the longitudinal and transverse resistances respectively.

Figs 4 and 5 [12] show corresponding results for silica-fume cement paste. The strain is essentially totally reversible in both the longitudinal and transverse directions, but the resistivity is only partly reversible in both directions, in contrast to the reversibility of the resistivity when fibers are present (Figs 2 and 3). As in the case with fibers, both longitudinal and transverse resistivities increase upon uniaxial tension. However, the gage factor is only 7.2 and −7.1 for Figs 4 and 5 respectively.

Comparison of Figs 2 and 3 (with fibers) with Figs 4 and 5 (without fibers) shows that fibers greatly enhance the magnitude and reversibility of the resistivity effect. The gage factors are much smaller in magnitude when fibers are absent.

The increase in both longitudinal and transverse resistivities upon uniaxial tension for cement pastes, whether with or without fibers, is attributed to defect (e.g., microcrack) generation. In the presence of fibers, fiber bridging across microcracks occurs and slight fiber pull-out occurs upon tension, thus enhancing the possibility of microcrack closing and causing more reversibility in the resistivity change. The fibers are much more electrically conductive than the cement matrix. The presence of the fibers introduces interfaces between fibers and matrix. The degradation of the fiber-matrix interface due to fiber pull-out or other mechanisms is an additional type of defect generation which will increase the resistivity of the composite. Therefore, the presence of fibers greatly increases the gage factor.

The transverse resistivity increases upon uniaxial tension, even though the Poisson Effect causes the transverse strain to be negative. This means that the effect of the transverse resistivity increase overshadows the effect of the transverse shrinkage. The resistivity increase is a consequence of the uniaxial tension. In contrast, under uniaxial compression, the resistance in the stress direction decreases at 28 days of curing. Hence, the effects of uniaxial tension on the transverse resistivity and of uniaxial compression on the longitudinal resistivity are different; the gage factors are negative and positive for these cases respectively.

The similarity of the resistivity change in longitudinal and transverse directions under uniaxial tension suggests similarity for other directions as well. This means that the resistance can be measured in any direction in order to sense the occurrence of tensile loading. Although the gage factor is comparable in both longitudinal and transverse directions, the fractional change in resistance under uniaxial tension is much higher in the longitudinal direction than the transverse direction. Thus, the use of the longitudinal resistance for practical self-sensing is preferred.

3. Cement-matrix composites for damage sensing

Concrete, whether with or without admixtures, is capable of sensing major and minor damage – even damage during elastic deformation – due to the electrical resistivity increase that accompanies damage [2, 6, 11, 18, 19]. That both strain and damage can be sensed simultaneously through resistance measurement means that the strain/stress condition (during dynamic loading) under which damage occurs can be obtained, thus facilitating damage origin identification. Damage is indicated by a resistance increase, which is larger and less reversible when the stress amplitude is higher. The resistance increase can be a sudden increase during loading. It can also be a gradual shift of the baseline resistance.

Fig. 6a [11] shows the fractional change in resistivity along the stress axis as well as the strain during

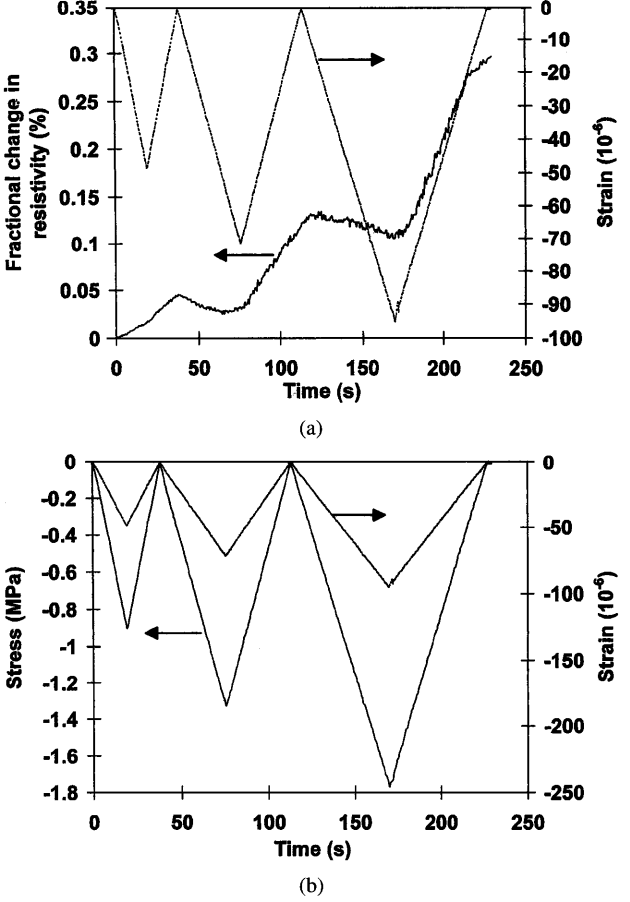

Figure 6 Variation of the fractional change in electrical resistivity with time (a), of the stress with time (b), and of the strain (negative for compressive strain) with time (a,b) during dynamic compressive loading at increasing stress amplitudes within the elastic regime for silica-fume cement paste at 28 days of curing.

repeated compressive loading at an increasing stress amplitude for plain cement paste at 28 days of curing. Fig. 6b [11] shows the corresponding variation of stress and strain during the repeated loading. The strain varies linearly with the stress up to the highest stress amplitude (Fig. 6b). The strain returns to zero at the end of each cycle of loading. During the first loading, the resistivity increases due to damage initiation. During the subsequent unloading, the resistivity continues to increase, probably due to opening of the microcracks generated during loading. During the second loading, the resistivity decreases slightly as the stress increases up to the maximum stress of the first cycle (probably due to closing of the microcracks) and then increases as the stress increases beyond this value (probably due to the generation of additional microcracks). During unloading in the second cycle, the resistivity increases significantly (probably due to opening of the microcracks). During the third loading, the resistivity essentially does not change (or decreases very slightly) as the stress increases to the maximum stress of the third cycle (probably due to the balance between microcrack generation and microcrack closing). Subsequent unloading causes the resistivity to increase very significantly (probably due to opening of the microcracks).

Fig. 7 [18] shows the fractional change in resistance, strain and stress during repeated compressive loading at

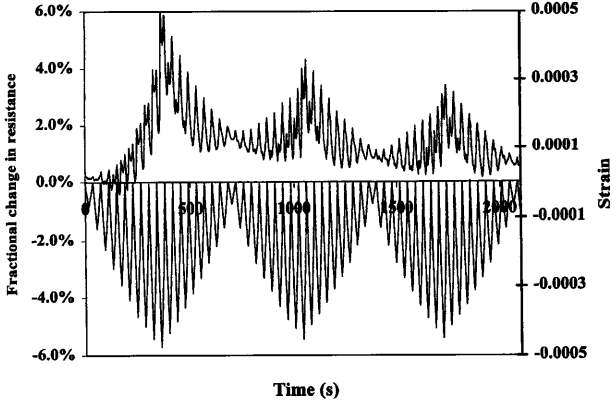

(a)

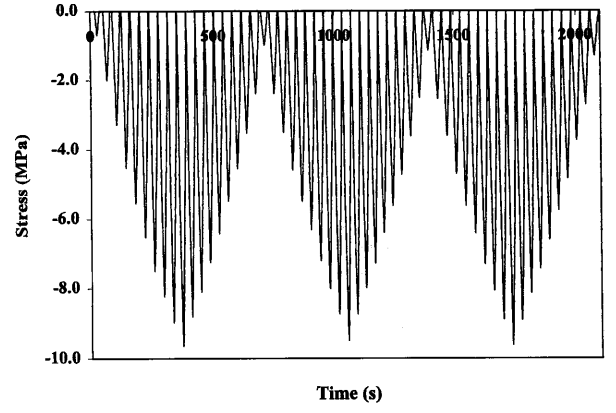

(b)

Figure 7 Fractional change in resistance (upper curve in (a)), strain (lower curve in (a)) and stress (b) during repeated compressive loading at increasing and decreasing stress amplitudes, the highest of which was 60% of the compressive strength, for carbon fiber concrete at 28 days of curing.

increasing and decreasing stress amplitudes for carbon fiber (0.18 vol.%) concrete (with fine and coarse aggregates) at 28 days of curing. The highest stress amplitude is 60% of the compressive strength. A group of cycles in which the stress amplitude increases cycle by cycle and then decreases cycle by cycle back to the initial low stress amplitude is hereby referred to as a group. Fig. 7 shows the results for three groups. The strain returns to zero at the end of each cycle for any of the stress amplitudes, indicating elastic behavior. The resistance decreases upon loading in each cycle, as in Fig. 1. An extra peak at the maximum stress of a cycle grows as the stress amplitude increases, resulting in two peaks per cycle. The original peak (strain induced) occurs at zero stress, while the extra peak (damage induced) occurs at the maximum stress. Hence, during loading from zero stress within a cycle, the resistance drops and then increases sharply, reaching the maximum resistance of the extra peak at the maximum stress of the cycle. Upon subsequent unloading, the resistance decreases and then increases as unloading continues, reaching the maximum resistance of the original peak at zero stress. In the part of this group where the stress amplitude decreases cycle by cycle, the extra peak diminishes and disappears, leaving the original peak as the sole peak. In the part of the second group where the stress amplitude increases cycle by cycle, the original peak (peak at zero stress) is the sole peak, except that the extra peak (peak at the maximum stress) returns in a minor way (more minor than in the first group) as the stress amplitude increases. The extra peak grows as the stress amplitude increases, but, in the part of the second group in which the stress amplitude decreases cycle by cycle, it quickly diminishes and vanishes, as in the first group. Within each group, the amplitude of resistance variation increases as the stress amplitude increases and decreases as the stress amplitude subsequently decreases.

The greater the stress amplitude, the larger and the less reversible is the damage-induced resistance increase (the extra peak). If the stress amplitude has been experienced before, the damage-induced resistance increase (the extra peak) is small, as shown by comparing the result of the second group with that of the first group (Fig. 7), unless the extent of damage is large (Fig. 8 for a highest stress amplitude of >90% the compressive strength). When the damage is extensive (as shown by a modulus decrease), damage-induced resistance increase occurs in every cycle, even at a decreasing stress amplitude, and it can overshadow the strain-induced resistance decrease (Fig. 8 [18]). Hence, the damage-induced resistance increase occurs mainly during loading (even within the elastic regime), particularly at a stress above that in prior cycles, unless the stress amplitude is high and/or damage is extensive.

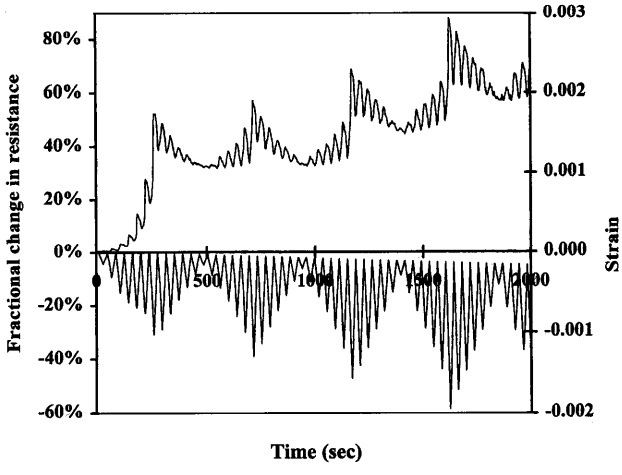

(a)

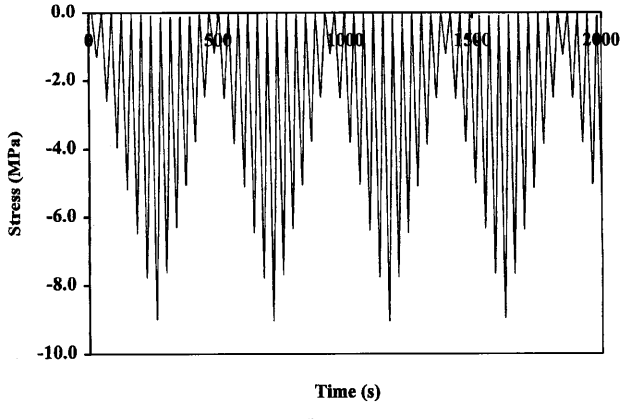

(b)

Figure 8 Fractional change in resistance (upper curve in (a)), strain (lower curve in (a)) and stress (b) during repeated compressive loading at increasing and decreasing stress amplitudes, the highest of which was >90% of the compressive strength, for carbon fiber concrete at 28 days of curing.

At a high stress amplitude, the damage-induced resistance increase cycle by cycle as the stress amplitude increases causes the baseline resistance to increase irreversibly (Fig. 8). The baseline resistance in the regime of major damage (with a decrease in modulus) provides a measure of the extent of damage (i.e., condition monitoring). This measure works in the loaded or unloaded state. In contrast, the measure using the damage-induced resistance increase (Fig. 7) works only during stress increase and indicates the occurrence of damage (whether minor or major) as well as the extent of damage.

4. Cement-matrix composites for temperature sensing

A thermistor is a thermometric device consisting of a material (typically a semiconductor, but in this case a cement paste) whose electrical resistivity changes with a variation in temperature. The carbon fiber concrete described in Sec. 2 for strain sensing is a thermistor due to its resistivity decreasing reversibly with increasing temperature [20]; the sensitivity is comparable to that of semiconductor thermistors. (The effect of temperature will need to be compensated in using the concrete as a strain sensor; Sec. 2.)

Fig. 9 [20] shows the current-voltage characteristic of carbon-fiber (0.5% by weight of cement) silica-fume (15% by weight of cement) cement paste at 38°C during stepped heating. The characteristic is linear below 5 V and deviates positively from linearity beyond 5 V. The resistivity is obtained from the slope of the linear portion. The voltage at which the characteristic starts to deviate from linearity is referred to as the critical voltage.

Fig. 10 shows a plot of the resistivity vs. temperature during heating and cooling for carbon-fiber silica-fume cement paste. The resistivity decreases upon heating and the effect is quite reversible upon cooling. That the resistivity is slightly increased after a heating-cooling cycle is probably due to thermal degradation of the material. Fig. 11 shows the Arrhenius plot of log conductivity (conductivity = 1/resistivity) vs. reciprocal absolute temperature. The slope of the plot gives the activation energy, which is 0.390 ± 0.014 and 0.412 ± 0.017 eV during heating and cooling respectively.

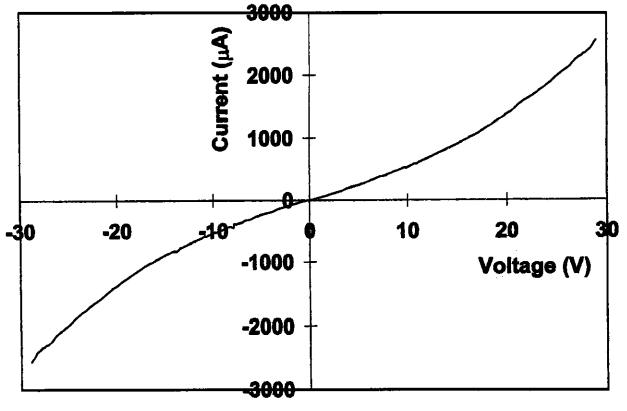

Figure 9 Current-voltage characteristic of carbon-fiber silica-fume cement paste at 38°C during stepped heating.

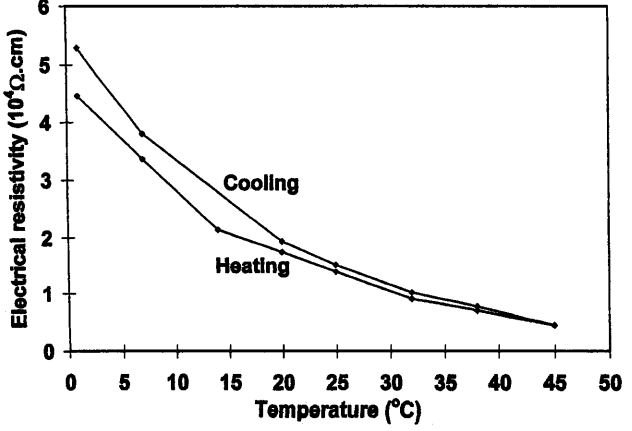

Figure 10 Plot of volume electrical resistivity vs. temperature during heating and cooling for carbon-fiber silica-fume cement paste.

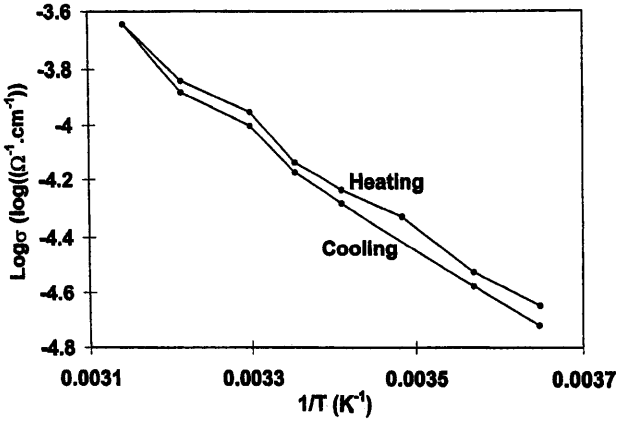

Figure 11 Arrhenius plot of log electrical conductivity vs. reciprocal absolute temperature for carbon-fiber silica-fume cement paste.

Results similar to those of carbon-fiber silica-fume cement paste were obtained with carbon-fiber (0.5% by weight of cement) latex (20% by weight of cement) cement paste, silica-fume cement paste, latex cement paste and plain cement paste. However, for all these four types of cement paste, (i) the resistivity is higher by about an order of magnitude, and (ii) the activation energy is lower by about an order of magnitude, as shown in Table I. The critical voltage is higher when fibers are absent (Table I).

The Seebeck [21–24] effect is a thermoelectric effect which is the basis for thermocouples for temperature measurement. This effect involves charge carriers moving from a hot point to a cold point within a material, thereby resulting in voltage difference between the two points. The Seebeck coefficient is the voltage difference per unit temperature difference between the two points. Negative carriers (electrons) make it more positive and positive carriers (holes) make it more negative.

The Seebeck effect in carbon fiber reinforced cement paste involves electrons from the cement matrix [23] and holes from the fibers [21, 22], such that the two contributions are equal at the percolation threshold, a fiber content between 0.5% and 1.0% by weight

TABLE I Resistivity, critical voltage and activation energy of five types of cement paste

Formulation	Resistivity at 20°C (Ω.cm)	Critical voltage at 20°C (V)	Activation energy (eV)	
			Heating	Cooling
Plain	$(4.87 \pm 0.37) \times 10^5$	10.80 ± 0.45	0.040 ± 0.006	0.122 ± 0.006
Silica fume	$(6.12 \pm 0.15) \times 10^5$	11.60 ± 0.37	0.035 ± 0.003	0.084 ± 0.004
Carbon fibers + silica fume	$(1.73 \pm 0.08) \times 10^4$	8.15 ± 0.34	0.390 ± 0.014	0.412 ± 0.017
Latex	$(6.99 \pm 0.12) \times 10^5$	11.80 ± 0.31	0.017 ± 0.001	0.025 ± 0.002
Carbon fibers + latex	$(9.64 \pm 0.08) \times 10^4$	8.76 ± 0.35	0.018 ± 0.001	0.027 ± 0.002

of cement [23]. The hole contribution increases monotonically with increasing fiber content below and above the percolation threshold [23].

Due to the free electrons in a metal, a cement containing metal fibers such as steel fibers is even more positive in the thermoelectric power than a cement without fibers [24]. The attainment of a very positive thermoelectric power is attractive, since a material with a positive thermoelectric power and a material with negative thermoelectric power are two very dissimilar materials, the junction of which is a thermocouple junction. (The greater the dissimilarity, the more sensitive is the thermocouple.)

Table II and Fig. 12 show the thermopower results. The absolute thermoelectric power is much more positive for all the steel-fiber cement pastes compared to all the carbon-fiber cement pastes. An increase of the steel fiber content from 0.5% to 1.0% by weight of cement increases the absolute thermoelectric power, whether silica fume (or latex) is present or not. An increase of the steel fiber content also increases the reversibility and linearity of the change in Seebeck voltage with the temperature difference between the hot and cold ends, as shown by comparing the values of the Seebeck coefficient obtained during heating and cooling in Table II. The values obtained during heating and cooling are close for the pastes with the higher steel fiber content, but are not so close for the pastes with the lower steel fiber content. In contrast, for pastes with carbon fibers in place of steel fibers, the change in Seebeck voltage with the temperature difference is highly reversible for both carbon fiber contents of 0.5% and 1.0% by weight of cement, as shown in Table II by comparing the values of the Seebeck coefficient obtained during heating and cooling.

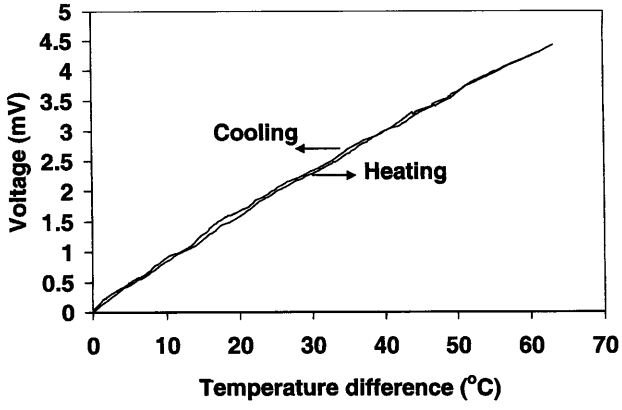

Figure 12 Variation of the Seebeck voltage (with copper as the reference) vs. the temperature difference during heating and cooling for steel-fiber silica-fume cement paste containing steel fibers in the amount of 1.0% by weight of cement.

Table II shows that the volume electrical resistivity is much higher for the steel-fiber cement pastes than the corresponding carbon fiber cement pastes. This is attributed to the much lower volume fraction of fibers in the former (Table II). An increase in the steel or carbon fiber content from 0.5% to 1.0% by weight of cement decreases the resistivity, though the decrease is more significant for the carbon fiber case than the steel fiber case. That the resistivity decrease is not large when the steel fiber content is increased from 0.5% to 1.0% by

TABLE II Volume electical resistivity, Seebeck coefficient (μV/°C) with copper as the reference, and the absolute thermoelectric power (μV/°C) of various cement pastes with steel fibers (S_f) or carbon fibers (C_f)

Cement paste	Volume fraction fibers	Resistivity (Ω.cm)	Heating		Cooling	
			Seebeck coefficient	Absolute thermoelectric power	Seebeck coefficient	Absolute thermoelectric power
S_f (0.5*)	0.10%	$(7.8 \pm 0.5) \times 10^4$	51.0 ± 4.8	53.3 ± 4.8	45.3 ± 4.4	47.6 ± 4.4
S_f (1.0*)	0.20%	$(4.8 \pm 0.4) \times 10^4$	56.8 ± 5.2	59.1 ± 5.2	53.7 ± 4.9	56.0 ± 4.9
S_f (0.5*) + SF	0.10%	$(5.6 \pm 0.5) \times 10^4$	54.8 ± 3.9	57.1 ± 3.9	52.9 ± 4.1	55.2 ± 4.1
S_f (1.0*) + SF	0.20%	$(3.2 \pm 0.3) \times 10^4$	66.2 ± 4.5	68.5 ± 4.5	65.6 ± 4.4	67.9 ± 4.4
S_f (0.5*) + L	0.085%	$(1.4 \pm 0.1) \times 10^5$	48.1 ± 3.2	50.4 ± 3.2	45.4 ± 2.9	47.7 ± 2.9
S_f (1.0*) + L	0.17%	$(1.1 \pm 0.1) \times 10^5$	55.4 ± 5.0	57.7 ± 5.0	54.2 ± 4.5	56.5 ± 4.5
C_f (0.5*) + SF	0.48%	$(1.5 \pm 0.1) \times 10^4$	-1.45 ± 0.09	0.89 ± 0.09	-1.45 ± 0.09	0.89 ± 0.09
C_f (1.0*) + SF	0.95%	$(8.3 \pm 0.5) \times 10^2$	-2.82 ± 0.11	-0.48 ± 0.11	-2.82 ± 0.11	-0.48 ± 0.11
C_f (0.5*) + L	0.41%	$(9.7 \pm 0.6) \times 10^4$	-1.20 ± 0.05	1.14 ± 0.05	-1.20 ± 0.05	1.14 ± 0.05
C_f (1.0*) + L	0.82%	$(1.8 \pm 0.2) \times 10^3$	-2.10 ± 0.08	0.24 ± 0.08	-2.10 ± 0.08	0.24 ± 0.08

* % by weight of cement.
SF: silica fume.
L: latex.

weight of cement and that the resistivity is still high at a steel fiber content of 1.0% by weight of cement suggest that a steel fiber content of 1.0% by weight of cement is below the percolation threshold.

Whether with or without silica fume (or latex), the change of the Seebeck voltage with temperature is more reversible and linear at a steel fiber content of 1.0% by weight of cement than at a steel fiber content of 0.5% by weight of cement. This is attributed to the larger role of the cement matrix at the lower steel fiber content and the contribution of the cement matrix to the irreversibility and non-linearity. Irreversibility and non-linearity are particularly significant when the cement paste contains no fiber.

From the practical point of view, the steel-fiber silica-fume cement paste containing steel fibers in the amount of 1.0% by weight of cement is particularly attractive for use in temperature sensing, as the absolute thermoelectric power is the highest (68 μV/°C) and the variation of the Seebeck voltage with the temperature difference between the hot and cold ends is reversible and linear. The absolute thermoelectric power is as high as those of commercial thermocouple materials.

Joints between concretes with different values of the thermoelectric power, as made by multiple pouring, provide concrete thermocouples [25].

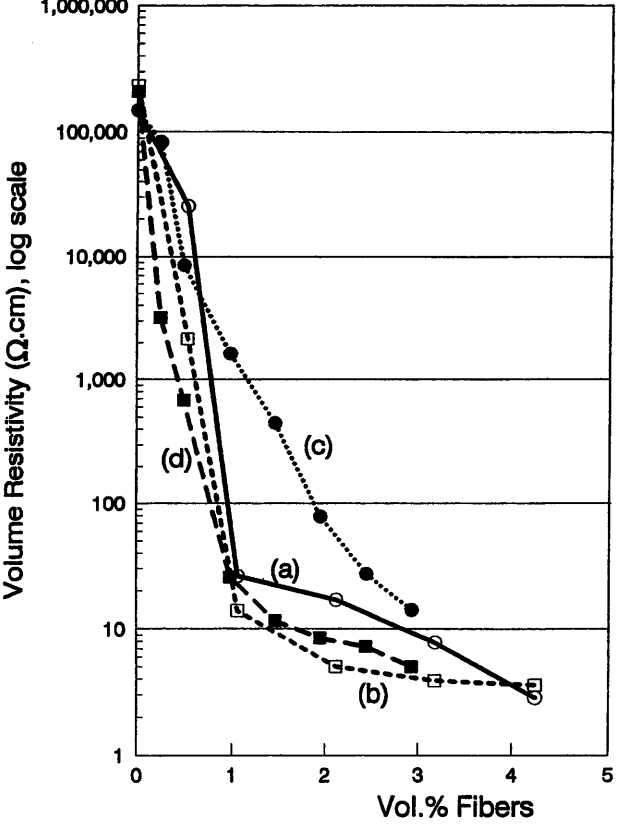

Figure 13 Variation of the volume electrical resistivity with carbon fiber volume fraction. (a) Without sand, with methylcellulose, without silica fume, (b) Without sand, with methylcellulose, with silica fume, (c) With sand, with methylcellulose, without silica fume, (d) With sand, with methylcellulose, with silica fume.

5. Cement-matrix composites for thermal control

Concretes that are inherently able to provide heating through Joule heating, provide temperature sensing (Sec. 4), or provide temperature stability through a high specific heat (high thermal mass) are highly desirable for thermal control of structures and energy saving in buildings. Concretes of low electrical resistivity [26–35] are useful for Joule heating, concrete thermistors and thermocouples are useful for temperature sensing, and concretes of high specific heat [36–39] are useful for heat retention. These concretes involve the use of admixtures such as fibers and silica fume. For example, silica fume introduces interfaces which promote the specific heat [36]; short carbon fibers enhance the electrical conductivity [31] and render the concrete p-type [23]. (Plain concrete is n-type electronically [23].) Comparative results shown in this section were obtained at similar moisture contents.

Fig. 13 [31] gives the volume electrical resistivity of composites at 7 days of curing. The resistivity decreases much with increasing fiber volume fraction, whether a second filler (silica fume or sand) is present or not. When sand is absent, the addition of silica fume decreases the resistivity at all carbon fiber volume fractions except the highest volume fraction of 4.24%; the decrease is most significant at the lowest fiber volume fraction of 0.53%. When sand is present, the addition of silica fume similarly decreases the resistivity, such that the decrease is most significant at fiber volume fractions below 1%. When silica fume is absent, the addition of sand decreases the resistivity only when the fiber volume fraction is below about 0.5%; at high fiber volume fractions, the addition of sand even increases the resistivity due to the porosity induced by the sand. Thus, the addition of a second filler (silica fume or sand) that is essentially non-conducting decreases the resistivity of the composite only at low volume fractions of the carbon fibers and the maximum fiber volume fraction for the resistivity to decrease is larger when the particle size of the filler is smaller. The resistivity decrease is attributed to the improved fiber dispersion due to the presence of the second filler. Consistent with the improved fiber dispersion is the increased flexural toughness and strength due to the presence of the second filler.

The specific heat is significantly increased by the addition of silica fume [37, 40]. It is further increased by the further addition of methylcellulose and defoamer. It is still further increased by the still further addition of carbon fibers. The effectiveness of the fibers in increasing the specific heat increases in the following order: as-received fibers, O_3-treated fibers, dichromate-treated fibers and silane-treated fibers. The highest specific heat is exhibited by the cement paste with silane-treated silica fume and silane-treated fibers. The specific heat is 12% higher than that of plain cement paste, 5% higher than that of the cement paste with as-received silica fume and as-received fibers, and 0.5% higher than that of the cement paste with as-received silica fume and silane-treated fibers. Hence, silane treatment of fibers is more valuable than that of silica fume for increasing the specific heat.

The thermal diffusivity is significantly decreased by the addition of silica fume [37, 40]. The further addition of methylcellulose and defoamer or the still

further addition of fibers has relatively little effect on the thermal diffusivity. Surface treatment of the fibers by ozone or dichromate slightly increases the thermal diffusivity, whereas surface treatment of the fibers by silane slightly decreases the thermal diffusivity. Silane treatments of silica fume and of fibers are about equally effective for lowering the thermal diffusivity.

The density is significantly decreased by the addition of silica fume [37, 40], which is used along with a water reducing agent. It is further decreased slightly by the further addition of methylcellulose and defoamer. It is still further decreased by the still further addition of fibers. The effectiveness of the fibers in decreasing the density decreases in the following order: as-received fibers, O_3-treated fibers, dichromate-treated fibers and silane-treated fibers. Silane treatment of fibers is more valuable than that of silica fume for increasing the density.

The thermal conductivity is significantly decreased by the addition of silica fume [37, 40]. The further addition of methylcellulose and defoamer or the still further addition of fibers has little effect on the density. Surface treatment of the fibers by ozone or dichromate slightly increases the thermal conductivity, whereas surface treatment of the fibers by silane has negligible effect. Silane treatments of silica fume and of fibers contribute comparably to reducing the thermal conductivity.

Sand is a much more common component in concrete than silica fume. It is different from silica fume in its relatively large particle size and negligible reactivity with cement. Sand gives effects that are opposite from those of silica fume, i.e., sand addition decreases the specific heat and increases the thermal conductivity [39].

Table III [39] shows the thermal behavior of cement pastes and mortars. Comparison of the results on cement paste without silica fume and those on mortar without silica fume shows that sand addition decreases the specific heat by 13% and increases the thermal conductivity by 9%. Comparison of the results on cement paste with silica fume and those on mortar with silica fume shows that sand addition decreases the specific heat by 11% and increases the thermal conductivity by 64%. That sand addition has more effect on the thermal conductivity when silica fume is present than when silica fume is absent is due to the low value of the thermal conductivity of cement paste with silica fume (Table III).

TABLE III Thermal behavior of cement pastes and mortars

	Cement paste		Mortar	
	Without silica fume*	With silica fume*	Without silica fume*	With silica fume*
Density (g/cm^3, ± 0.02)	2.01	1.73	2.04	2.20
Specific heat (J/g.K, ± 0.001)	0.736	0.788	0.642	0.705
Thermal diffusivity (mm^2/s, ± 0.03)	0.36	0.24	0.44	0.35
Thermal conductivity§ (W/m.K, ± 0.03)	0.53	0.33	0.58	0.54

*Silane treated.
§Product of density, specific heat and thermal diffusivity.

Comparison of the results on cement paste without silica fume and on cement paste with silica fume shows that silica fume addition increases the specific heat by 7% and decreases the thermal conductivity by 38%. Comparison of the results on mortar without silica fume and on mortar with silica fume shows that silica fume addition increases the specific heat by 10% and decreases the thermal conductivity by 6%. Hence, the effects of silica fume addition on mortar and cement paste are in the same directions. That the effect of silica fume on the thermal conductivity is much less for mortar than for cement paste is mainly due to the fact that silica fume addition increases the density of mortar but decreases the density of cement paste (Table III). That the fractional increase in specific heat due to silica fume addition is higher for mortar than cement paste is attributed to the low value of the specific heat of mortar without silica fume (Table III).

Comparison of the results on cement paste with silica fume and those on mortar without silica fume shows that sand addition gives a lower specific heat than silica fume addition and a higher thermal conductivity than silica fume addition. Since sand has a much larger particle size than silica fume, sand results in much less interface area than silica fume, though the interface may be more diffuse for silica fume than for sand. The low interface area in the sand case is believed to be responsible for the low specific heat and the higher thermal conductivity, as slippage at the interface contributes to the specific heat and the interface acts as a thermal barrier.

Silica fume addition increases the specific heat of cement paste by 7%, whereas sand addition decreases it by 13%. Silica fume addition decreases the thermal conductivity of cement paste by 38%, whereas sand addition increases it by 22%. Hence, silica fume addition and sand addition have opposite effects. The cause is believed to be mainly associated with the low interface area for the sand case and the high interface area for the silica fume case, as explained in the last paragraph. The high reactivity of silica fume compared to sand may contribute to causing the observed difference between silica fume addition and sand addition, though this contribution is believed to be minor, as the reactivity should have tightened up the interface, thus decreasing the specific heat (in contrast to the observed effects). The decrease in specific heat and the increase in thermal conductivity upon sand addition are believed to be due to the higher level of homogeneity within a sand particle than within cement paste.

6. Cement-matrix composites for vibration reduction

Vibration reduction requires a high damping capacity and a high stiffness. Viscoelastic materials such as rubber have a high damping capacity but a low stiffness. Concretes having both high damping capacity (two or more orders higher than conventional concrete) (Table IV) [41] and high stiffness (Table V) [41] can

TABLE IV Loss tangent (tan δ)

Mix	0.2 Hz	0.5 Hz	1.0 Hz	2.0 Hz
Plain*	0.016 ± 0.01	$<10^{-4}$	$<10^{-4}$	$<10^{-4}$
Sand	$<10^{-4}$	$<10^{-4}$	$<10^{-4}$	$<10^{-4}$
Sand + silica fume	0.021 ± 0.01	0.14 ± 0.01	0.01 ± 0.01	$<10^{-4}$

*No sand, no silica fume.

TABLE V Storage modulus (GPa, ± 0.2)

Mix	0.2 Hz	0.5 Hz	1.0 Hz	2.0 Hz
Plain*	13.7	14.48	14.02	14.00
Sand	9.43	11.67	10.32	9.56
Sand + silica fume	13.11	14.34	13.17	13.11

*No sand, no silica fume.

be obtained by using surface treated silica fume as an admixture in the concrete. Steel reinforced concretes having improved damping capacity and stiffness can be obtained by surface treating the steel (say by sand blasting) prior to incorporating the steel in the concrete (Table VI) [42], or by using silica fume in the concrete [41]. Due to its small particle size, silica fume in concrete introduces interfaces which enhance damping. Sand blasting of a steel rebar increases the interface area between steel and concrete, thereby enhancing damping. Carbon fiber addition has relatively small effects on the damping capacity and stiffness [43].

7. Cement-matrix composites for reflecting electromagnetic radiation

Cement-matrix composites containing 0.1 μm diameter discontinuous carbon filaments are effective for reflecting radio waves [44]. Due to the skin effect, conventional carbon fibers (7–15 μm diameter) are much less effective. The reflectivity renders the ability to shield EMI and to provide lateral guidance in the automatic highway technology [44].

8. Conclusion

By the use of admixtures such as short carbon fibers, short steel fibers and silica fume, cement-matrix composites were rendered multifunctionality. The functions include strain sensing, damage sensing, temperature sensing, thermal control, vibration reduction and radio wave reflection.

Acknowledgement

This work was supported in part by National Science Foundation, U.S.A.

References

1. X. FU, W. LU and D. D. L. CHUNG, *Carbon* **36**(9) (1998) 1337.
2. P. CHEN and D. D. L. CHUNG, *Smart Mater. Struct.* **2** (1993) 22.
3. *Idem., Composites*, Part B **27B** (1996) 11.
4. *Idem., J. Amer. Ceram. Soc.* **78**(3) (1995) 816.
5. D. D. L. CHUNG, *Smart Mater. Struct.* **4** (1995) 59.
6. P. CHEN and D. D. L. CHUNG, *ACI Mater. J.* **93**(4) (1996) 341.
7. X. FU and D. D. L. CHUNG, *Cem. Concr. Res.* **26**(1) (1996) 15.
8. X. FU, E. MA, D. D. L. CHUNG and W. A. ANDERSON, *ibid.* **27**(6) (1997) 845.
9. X. FU and D. D. L. CHUNG, *ibid.* **27**(9) (1997) 1313.
10. X. FU, W. LU and D. D. L. CHUNG, *ibid.* **28**(2) (1998) 183.
11. S. WEN and D. D. L. CHUNG, *Cem. Concr. Res.*, in press.
12. *Idem., Cem. Concr. Res.* **30**(8) (2000) 1289.
13. Z. SHI and D. D. L. CHUNG, *ibid.* **29**(3) (1999) 435.
14. Q. MAO, B. ZHAO, D. SHENG and Z. LI, *J. Wuhan Univ. Tech., Mater. Sci. Ed.* **11**(3) (1996) 41.
15. Q. MAO, B. ZHAO, D. SHEN and Z. LI, *Fuhe Cailiao Xuebao/Acta Materiae Compositae Sinica* **13**(4) (1996) 8.
16. M. SUN, Q. MAO and Z. LI, *J. Wuhan Univ. Tech., Mater. Sci. Ed.* **13**(4) (1998) 58.
17. B. ZHAO, Z. LI and D. WU, *ibid.* **10**(4) (1995) 52.
18. D. BONTEA, D. D. L. CHUNG and G. C. LEE, *Cem. Concr. Res.* **30**(4) (2000) 651.
19. J. LEE and G. BASTON, in Materials for the New Millennium, Proceedings of the 4th Materials Engineering Conference, Vol. 2, 1996 (ASCE, New York, NY, 1996) p. 887.
20. S. WEN and D. D. L. CHUNG, *Cem. Concr. Res.* **29**(6) (1999) 961.

TABLE VI Loss tangent, storage modulus and loss modulus of mortars with and without steel reinforcement

Property	Sample type	Frequency		
		0.2 Hz	0.5 Hz	1.0 Hz
Loss tangent	A	$<10^{-4}$	$<10^{-4}$	$<10^{-4}$
	B	$(2.73 \pm 0.19) \times 10^{-2}$	$(1.56 \pm 0.08) \times 10^{-2}$	$(7.20 \pm 0.37) \times 10^{-3}$
	C	$(3.32 \pm 0.15) \times 10^{-2}$	$(1.98 \pm 0.17) \times 10^{-2}$	$(1.07 \pm 0.09) \times 10^{-2}$
	D	$(3.65 \pm 0.27) \times 10^{-2}$	$(2.50 \pm 0.22) \times 10^{-2}$	$(1.24 \pm 0.16) \times 10^{-2}$
Storage modulus (GPa)	A	20.2 ± 3.5	27.5 ± 4.3	25.8 ± 3.7
	B	44.2 ± 4.8	47.7 ± 5.3	44.4 ± 5.0
	C	36.9 ± 4.3	41.0 ± 3.9	38.4 ± 3.0
	D	46.0 ± 4.0	51.2 ± 6.4	49.3 ± 5.8
Loss modulus (GPa)	A	$<10^{-3}$	$<10^{-3}$	$<10^{-3}$
	B	1.21 ± 0.22	0.74 ± 0.12	0.32 ± 0.05
	C	1.23 ± 0.20	0.81 ± 0.15	0.41 ± 0.07
	D	1.68 ± 0.27	1.28 ± 0.27	0.61 ± 0.51

Note on sample type designations.
A: No rebar.
B: As-received steel rebar.
C: Ozone treated steel rebar.
D: Sand blasted steel rebar.

21. M. SUN, Z. LI, Q. MAO and D. SHEN, *ibid.* **28**(4) (1998) 549.
22. *Idem.*, *ibid.* **28**(12) (1998) 1707.
23. S. WEN and D. D. L. CHUNG, *ibid.* **29**(12) (1999) 1989.
24. *Idem.*, *ibid.* **30**(4) (2000) 661.
25. *Idem.*, *ibid.* in press.
26. X. FU and D. D. L. CHUNG, *ibid.* **25**(4) (1995) 689.
27. J. HOU and D. D. L. CHUNG, *ibid.* **27**(5) (1997) 649.
28. G. G. CLEMENA, *Materials Performance* **27**(3) (1988) 19.
29. R. J. BROUSSEAU and G. B. PYE, *ACI Mater. J.* **94**(4) (1997) 306.
30. P. CHEN and D. D. L. CHUNG, *Smart Mater. Struct.* **2** (1993) 181.
31. *Idem.*, *J. Electron. Mater.* **24**(1) (1995) 47.
32. X. WANG, Y. WANG and Z. JIN, *Fuhe Cailiao Xuebao/Acta Materiae Compositae Sinica* **15**(3) (1998) 75.
33. N. BANTHIA, S. DJERIDANE and M. PIGEON, *Cem. Concr. Res.* **22**(5) (1992) 804.
34. P. XIE, P. GU and J. J. BEAUDOIN, *J. Mater. Sci.* **31**(15) (1996) 4093.
35. Z. SHUI, J. LI, F. HUANG and D. YANG, *J. Wuhan Univ. Tech., Mater. Sci. Ed.* **10**(4) (1995) 37.
36. X. FU and D. D. L. CHUNG, *ACI Mater. J.* **96**(4) (1999) 455.
37. Y. XU and D. D. L. CHUNG, *Cem. Concr. Res.* **29**(7) (1999) 1117.
38. Y. SHINOZAKI, in Proc. 22nd National SAMPE Tech. Conf. Vol. 22, 1990 (SAMPE, Covina, CA, 1990) p. 986.
39. Y. XU and D. D. L. CHUNG, *Cem. Concr. Res.* **30**(1) (2000) 59.
40. *Idem.*, *ACI Mater. J.* **97**(3) (2000) 333.
41. Y. WANG and D. D. L. CHUNG, *Cem. Concr. Res.* **28**(10) (1998) 1353.
42. S. WEN and D. D. L. CHUNG, *ibid.* **30**(2) (2000) 327.
43. Y. XU and D. D. L. CHUNG, *ibid.* **29**(7) (1999) 1107.
44. X. FU and D. D. L. CHUNG, *Carbon* **36**(4) (1998) 459.

Received 5 March
and accepted 21 July 2000